






A Detailed Analysis of the Association between Urate Deposition and Erosions and Osteophytes in Gout

Caroline Pecherstorfer,¹  David Simon,¹  Sara Unbehend,¹ Hanna Ellmann,¹ Matthias Englbrecht,¹ Fabian Hartmann,¹ Camille Figueiredo,² Axel Hueber,¹ Judith Haschka,³ Roland Kocijan,⁴ Arnd Kleyer,¹  Georg Schett,¹  Jürgen Rech,¹  and Sara Bayat¹

Objective. To characterize in detail the structural bone changes associated with the deposition of monosodium urate crystals in the first metatarsophalangeal (MTP1) joint in patients with tophaceous gout.

Methods. Twenty patients with tophaceous gout and involvement of the MTP1 joint received both dual-energy computed tomography (DECT) of the feet for the detection of tophi and high-resolution peripheral quantitative computed tomography (HR-pQCT) of the feet for the detection of bone erosions and osteophytes. Demographic and clinical data were collected. Tophi in DECT and erosions and osteophytes in HR-pQCT were overlaid to define their anatomical relation. In addition, the feet of 20 sex- and age-matched healthy controls were scanned to define the normal architecture of the MTP1 joint.

Results. Patients with gout had an increased number and extent of bone erosions and osteophytes compared with their healthy counterparts (erosions: 5 [0-17] vs 1 [1-2], 45.32 mm³ [7.26-550.32] vs 0.82 mm³ [0.15-21.8]; osteophytes: 10.5 [0-26] vs 1 [0-10], 4.93 mm [0.77-7.19 mm] vs 0.93 mm [0.05-7.61 mm]; all $P < 0.001$). The median tophi volume detected by DECT (0.12 mm³ [0.01-2.53]) was highly associated with the total volume of erosions ($r = 0.597$, $P = 0.005$).

Conclusion. Gout patients show increased changes in their bone microarchitecture. The extent of uric acid deposition is positively correlated with the extent of bone loss at the MTP1 joint, highlighting the strong cohesion of inflammation and erosive changes.

INTRODUCTION

Gout is one of the most common inflammatory diseases, with a prevalence between 1.4% and 3.9% in Western countries (1,2). It more frequently affects males and is associated with the deposition of monosodium urate (MSU) crystals in the joints, tendons, and entheses (1,2). Crystals form on the basis of supersaturated concentrations of uric acid in the extracellular fluid. Increase of uric acid level is especially found with the age- or disease-mediated decline of kidney function, the chronic ingestion of purine-rich food, or cell lysis during cancer or excessive fasting, all of which can lead to increased purine release from dying cells. Upon their formation, MSU crystals are recognized as danger signals by the

immune system and lead to acute inflammation, which is largely driven by the influx of innate immune cells, such as neutrophils and monocytes, to the affected sites (2).

Clinical data suggest that gout has bone-destructive features (3,4). In radiographic studies using plain radiography or scanning by conventional clinical computed tomography (CT), bone erosion and osteophytes were detected in patients with chronic gout (3,5). These structural changes were evaluated using semiquantitative methods, such as the modified Sharp/van der Heijde system or adapted Rheumatoid Arthritis Magnetic Resonance Imaging Score (3,6,7). It has been demonstrated that these methods are reliable in detecting erosive changes and are suitable for quantifying the extent of destruction indirectly (8). Apart from this, several

Presented by Caroline Pecherstorfer in fulfillment of the requirements for an MD degree, Friedrich Alexander University Erlangen-Nuremberg.

¹Caroline Pecherstorfer, David Simon, Sara Unbehend, Hanna Ellmann, Matthias Englbrecht, Fabian Hartmann, Axel Hueber, Arnd Kleyer, Georg Schett, Jürgen Rech, Sara Bayat: Friedrich-Alexander-University Erlangen-Nuremberg and Universitätsklinikum Erlangen, Erlangen, Germany; ²Camille Figueiredo: Faculdade de Medicina da Universidade de São Paulo, São Paulo, Brazil; ³Judith Haschka: St. Vincent Hospital, Vienna, Austria and Academic Teaching Hospital of Medical University of Vienna, Vienna, Austria; ⁴Roland Kocijan: Ludwig Boltzmann Institute of Osteology at Hanusch Hospital of

OEGK and AUVA Trauma Centre Meidling, 1st Medical Department Hanusch Hospital, Vienna, Austria.

Drs. Pecherstorfer and Simon contributed equally to this work; Drs. Rech and Bayat contributed equally to this work.

The authors have declared no conflicts of interest.

Address correspondence to Georg Schett, MD, Department of Internal Medicine 3, Friedrich Alexander University Erlangen-Nuremberg and Universitätsklinikum Erlangen Ulmenweg 18, 91054 Erlangen, Germany. E-mail: georg.schett@uk-erlangen.de.

Submitted for publication December 9, 2019; accepted in revised form July 21, 2020.

studies have suggested that urate deposition is a key factor associated with bone erosions (3,5,6,9). Dalbeth et al demonstrated that the deposition of MSU crystals is associated with erosive changes, whereas Shi et al additionally showed that the volume of MSU crystals correlates positively with erosion volume (3,9). However, those data on quantification of erosions are based only on dual-energy CT (DECT) technology (9). A more precise imaging tool is high-resolution peripheral quantitative CT (HR-pQCT), which can detect catabolic and anabolic bone changes very accurately. HR-pQCT has been shown to be able to exactly localize and measure bone erosions smaller than 0.5 mm in width or depth as well as bony spurs in patients with arthritis (10–12). Therefore, HR-pQCT could, for the first time, be used for in-depth detailed assessment of the relationship between erosions as well as osteophytes with urate deposits in tophaceous gout patients (10,11).

Consequently, in this hypothesis-generating study, we focused on patients with gout of the hallux and performed DECT and HR-pQCT scanning to investigate in detail the association between urate deposition with erosions and osteophytes.

PATIENTS AND METHODS

Patients. Patients with gout were recruited from the Department of Internal Medicine 3 of the University of Erlangen-Nuremberg. Strict inclusion criteria of the study for patients with gout were in fulfillment of the ACR/EULAR classification criteria of gout (13), absence of any other rheumatic disease, and chronic tophaceous gout of the first metatarsophalangeal (MTP1) joint proven by DECT (13). We screened 100 patients with gout to obtain 20

patients with tophaceous DECT-positive gout of the MTP1 joint. All patients received DECT and HR-pQCT scans of the MTP1 joint. To compare the results on bone structure obtained by HR-pQCT, sex- and age-adjusted healthy controls also underwent HR-pQCT.

Demographic data (sex, age, and body mass index), clinical data (duration of gout, 68-tender joint count, 66-swollen joint count, pain by visual analogue scale [VAS], health assessment questionnaire–disability index [HAQ-DI]), and laboratory findings (C-reactive protein, serum uric acid level) as well as data on the current treatment of gout were recorded. We also collected data on the presence of hypertension, diabetes mellitus, and renal disease.

Healthy subjects were recruited through a prospective field campaign through advertisements and flyers. Exclusion criteria for healthy subjects were a history of arthritis or any other musculoskeletal disease; osteoporosis or pathological fractures; liver, kidney, or heart diseases; metabolic diseases including diabetes mellitus or thyroiditis; and treatments with glucocorticoids or bisphosphonates. To obtain 20 healthy controls, we had to screen 32 subjects.

The study was approved by the Ethics Committee of the Medical University Erlangen-Nuremberg. Written informed consent was obtained from each patient, and the study was conducted in accordance with the declaration of Helsinki.

Dual-energy CT. All 20 patients with gout were examined by a dual X-ray tube 128-detector row scanner (Somatom Definition Flash, Siemens Medical). Healthy controls did not receive DECT because they were not expected to have tophi. The patients were positioned feet-first in a supine position, with the feet in a plantar

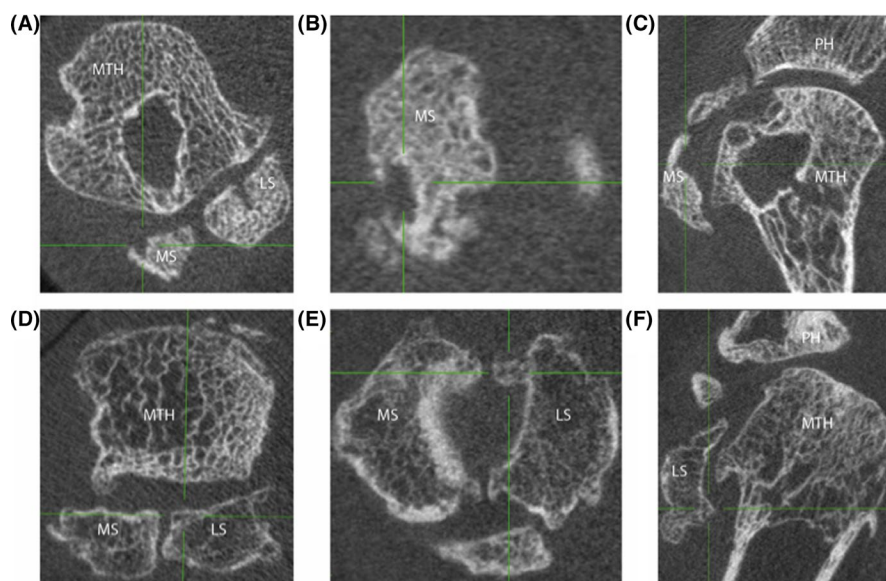


Figure 1. Method used to analyze structural bone damage in the metatarsophalangeal joint I of patients with gout using high-resolution peripheral quantitative computed tomography (HR-pQCT). HR-pQCT of the first metatarsophalangeal joints showing erosions (top) and osteophytes (bottom). From left to right coronal, axial, and sagittal views are shown. Target lesions are indicated by green lines in all three planes. Abbreviations: D, distal; L, lateral; LS, lateral sesamoid bone; M, medial; MS, medial sesamoid bone; MTH, metatarsal head I; P, proximal; PHI, phalangeal base I. [Color figure can be viewed at wileyonlinelibrary.com]

flexion position (14). They were scanned in craniocaudal direction—5 cm from the ankle joint to the tips of the toes (14). All scans were performed axially with an acquisition at 128×0.6 mm and pitch of 0.7 (14). X-ray tube number 1 was operated at 80 kV/260 mA and tube number 2 at 140 kV/130 mA (14).

Analysis of DECT images. Analysis of DECT images was performed on a proprietary workstation (MultiModality Workspace, Siemens Medical) with proprietary software (Syngo DE Gout #MM, Siemens Medical) (14). We originally used a semi-quantitative scoring system to measure the severity of urate depositions, but this proved impracticable for our purposes as 90% of our test group ranked in the top-most category (the method is described elsewhere in detail (14)). We subsequently manually outlined urate depositions at the MTP1 joint; tophi volumes (in millimeters cubed) were then calculated using an automated volume assessment software (Syngo volume calculation) (14). Analysis and scoring were performed by two independent and blinded readers (HE and SB)

High-resolution peripheral quantitative CT. HR-pQCT scans of both the metatarsophalangeal joints of gout patients and healthy controls were performed using an Xtreme CT I scanner (SCANCO Medical). The high-resolution technique offers a

three-dimensional, noninvasive depiction of cortical and trabecular bone structure with a standard digital isotropic resolution of up to $82 \times 82 \times 82$ μm voxel size and low radiation exposure under 3 μS (10–12). Patients lay prone with their lower legs in slight dorsal flexion. The selected foot was fixed in a leg splint and placed into the HR-pQCT from ankle to toes. Measurements lasted 8 minutes. A total of 296 slices were taken in proximal-to-distal direction from the base of metatarsophalangeal joints to the tip of the toes. HR-pQCT scans were performed with a nominal resolution of $123 \mu\text{m}^3$.

HR-pQCT analysis. HR-pQCT images were assessed for bone erosions and osteophytes. Bone erosions were defined as pathological juxta-articular cortical break, at least traceable in two successive slices and in two vertical planes (10). Osteophytes were defined as protrusions of the cortical pattern and had to be at least traceable in two sequential slices and in two perpendicular planes. The MTP1 joint as well as the phalangeal base were separated into four quadrants. Those eight quadrants and the two sesamoid bones were assessed for structural lesions (Figure 1). Presence of erosions and osteophytes were identified by two independent and blinded readers (CP and SU).

A threshold-based segmentation (lower threshold 0, upper threshold 109) method for volumetric measurement of bone

Table 1. Demographic and clinical characteristics

	Gout	Controls	<i>P</i> value
Number of subjects	20	20	
Sex (male/female)	15/5	12/8	0.31
Age (y)	58.7 \pm 10.3	54.2 \pm 9.6	0.16
Height (cm)	174.9 \pm 9.1	172.6 \pm 8.3	0.24
Weight (kg)	87.3 \pm 23.4	80.3 \pm 19.4	0.31
BMI	28.2 \pm 6.3	26.7 \pm 4.4	0.30
Alcohol ingestion, N (%)	13 (65.0)	12 (60.0)	0.74
Smokers, N (%)	9 (45.0)	7 (35.0)	0.52
Comorbidities			
Hypertension, N (%)	12 (60)	3 (15)	0.008
Chronic renal disease, N (%)	5 (25)	0 (0)	0.047
Diabetes, N (%)	1 (5)	0 (0)	>0.99
Chronic heart disease, N (%)	1 (5)	1 (5)	>0.99
Disease-specific characteristics			
Duration of gout (y)	12.1 \pm 8.3
Musculoskeletal symptoms			
Tender joint count 68 (N)	2.5 \pm 3.6
Swollen joint count 66 (N)	0.6 \pm 1.4
VAS pain (mm)	4.1 \pm 5.4
HAQ-DI score (units)	0.6 \pm 0.7
Laboratory parameters			
Uric acid (mg/L)	5.8 \pm 2.7
C-reactive protein (mg/L)	7.2 \pm 11.8
Treatment modalities			
Allopurinol, N (%)	6 (30.0)
Febuxostat, N (%)	10 (50.0)
Pegloticase, N (%)	1 (5.0)
Uricosuric drugs, N (%)	1 (5.0)
No medication	4 (20.0)

Note. All continuous parameters are shown in mean \pm SD. Abbreviations: BMI, body mass index; HAQ-DI, health assessment questionnaire–disability index; VAS, visual analogue scale.

erosion was used. Lesions were manually contoured slice by slice to ensure the whole bone lesion was covered (15,16). After that, a graphical object (gobj) was created and was used to calculate the bone erosion volume (15,16). Protrusions were measured from the cortical base to the top of the protrusion. The biggest osteophyte per quadrant was used for volumes calculations. The process is described in detail elsewhere (11). All described steps were performed using the open access viewer OsiriX (version 5.8.22) and SCANCO Medical Xtreme CT software (version 6.0) (15,16).

Statistical analyses. SPSS (version 23.0.0; IBM SPSS statistics) was used for statistical analyses. We applied Mann-Whitney *U* test in order to investigate potential differences with respect to continuous sample characteristics. Differences with respect to frequency distributions of categorical variables were tested using the χ^2 test. Spearman correlation coefficients were used to investigate the relation between tophus volume and erosion volume. Values are expressed as medians (minimum to maximum), demographic data are illustrated as means and SD. Interreader reliability was tested using intraclass correlation coefficients (2 κ).

RESULTS

Demographic and clinical data. A total of 20 patients with gout (15 males, 5 females; age: 58.7 ± 10.3 years) and 20 healthy controls (12 males, 8 females; age: 54.2 ± 9.6 years) were analyzed. There was no significant difference between the two

groups with regard to sex ($p = 0.31$), age ($P = 0.16$), body mass index ($P = 0.30$), alcohol ingestion ($P = 0.74$), and smoking ($P = 0.52$). The mean duration of gout was 12.1 ± 8.3 years. All but two patients received uric acid-lowering treatment, mostly with xanthine oxidase blockers. Mean \pm SD serum urate level was low at 5.8 ± 2.7 mg/L. Demographic and disease-specific characteristics are shown in Table 1.

Analysis of tophus burden. DECT analysis revealed a median tophus volume measured 0.12 mm^3 (0.01-2.53) in the MTP1 joint. Based on the previously published semiquantitative scoring system of urate deposition (6), 18 of 20 patients fell into the highest grade of tophus burden (score 3; range of score: 0-3). There was no significant difference between females and males with respect to tophus volume ($P = 0.142$). All 20 gout patients presented tophi in the medial compartment of the metatarsal head. Interrater reliability of tophi was 1.0.

Analysis of structural bone lesions. HR-pQCT analysis showed that patients with gout had a significantly higher number of erosions and osteophytes than healthy controls. Hence, the median number of erosions in the MTP1 joint was 5 ($n = 0-17$) in gout patients and 1 ($n = 1-2$) in healthy controls ($P < 0.001$) (Figure 2A). Furthermore, the median erosion volume was 45.3 mm^3 ($n = 7.2-550.3$) in patients with gout compared with 0.82 mm^3 ($n = 0.15-21.8$) in healthy controls ($P < 0.001$) (Figure 2B). Interrater reliability of the number of bone erosions was 0.90 (95%

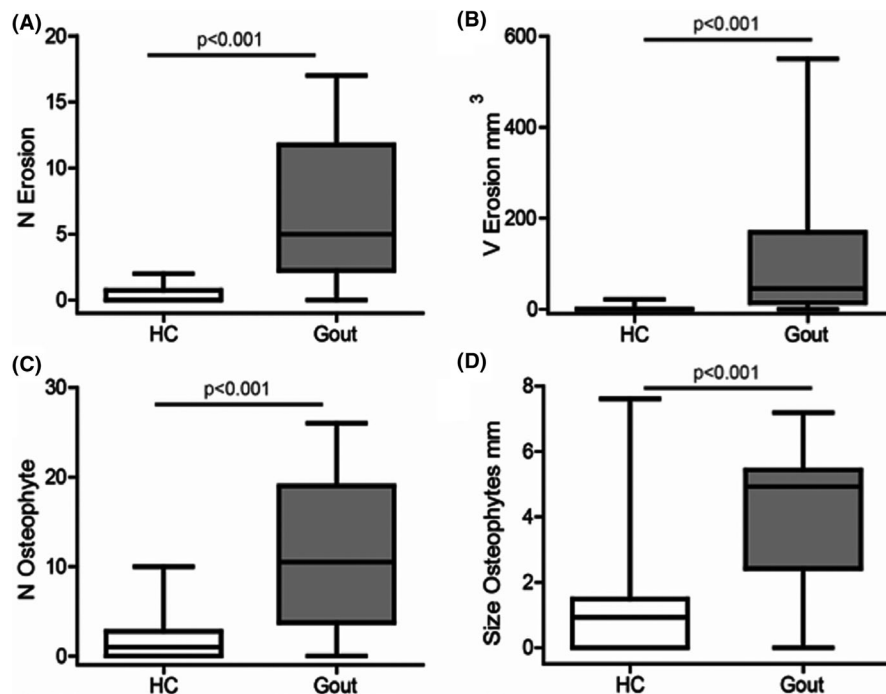


Figure 2. Quantification of bone erosions and osteophytes in patients with gout and healthy controls (HC). Data are based on high-resolution peripheral quantitative computed tomography of first metatarsophalangeal joints in patients with gout (gray boxplots) and HCs (white boxplots); number (N) of bone erosions (A), volume (V) of bone erosions (B), number (N) of osteophytes (C), and size of osteophytes (D). Data are shown as medians and interquartile ranges (boxes).

confidence interval [CI]: 0.75, 0.95), and for bone erosion volume it was 0.89 (95% CI: 0.79, 0.94). With respect to osteophytes, the median number of osteophytes was 10.5 (range = 0-26) and 1 (range = 0-10) in gout and healthy controls ($P < 0.001$), respectively (Figure 2C). Median size of osteophytes was 4.93 mm (range = 0.77-7.19) and 0.93 mm (range = 0.05-7.61) in the gout and healthy control groups, respectively ($P < 0.001$) (Figure 2D). Interrater reliability for osteophytes number was 0.91 (95% CI: 0.77, 0.95) and for their size it was 0.97 (95% CI: 0.94, 0.98).

Distribution of bone erosions and osteophytes.

The dominant site for bone erosions was the medial side of the metatarsal head, which was observed in 75% of the cases (Figure 3). After the metatarsal head, the medial sesamoid bone and the medial phalangeal base, which were each involved in 45% of the patients, were other predilection sites. Also, the volume analysis of bone erosions showed that the medial side of the metatarsal head and the medial sesamoid bone are the most severely affected sites. Notably, the distribution of bone erosions was reflected the distribution of DECT-based urate deposition. Osteophytes were more evenly distributed and affected the entire circumference of the MTP1 joint. The dorsal site was the MTP1 joint compartment most prone to developing osteophytes. In patients with gout, the burden of bone erosions

was well correlated with the burden of osteophytes ($r = 0.713$, $P < 0.001$). Results for the distribution of bone erosions and osteophytes in the healthy control group were similar with preferential affection of the medial metatarsal heads and sesamoid bones for bone erosions and a more even distribution for osteophytes, albeit both lesions showed a much lower prevalence than in gout patients.

Relation between urate burden and structural bone lesions. We next addressed whether the degree of urate deposition is related to the extent of structural damage. There was a significant correlation between tophus volume and bone erosion volume ($r = 0.597$, $P = 0.005$), whereas no significant correlation was found with the number and sizes of the osteophytes. These findings are also reflected by the overlay of DECT and HR-pQCT images, which showed that erosions develop in direct vicinity to urate depositions, whereas osteophytes develop in direct vicinity to the erosive lesions (Figure 4).

DISCUSSION

This study provides new, very detailed insights into the relation between tophus formation and structural bone damage in gout. Analyses were performed in the MTP1 joint, which is the most

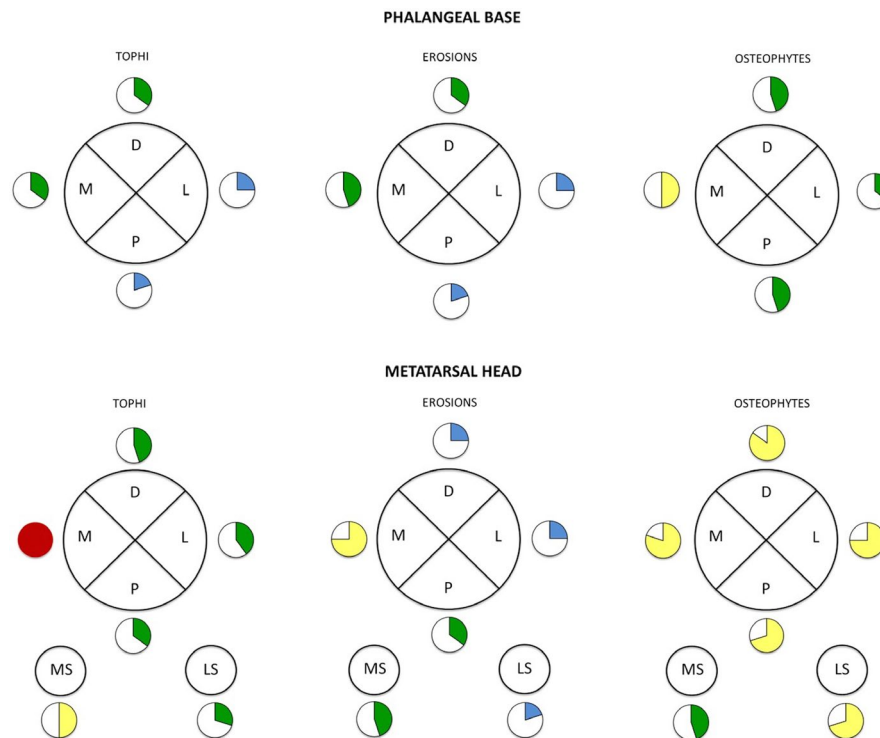


Figure 3. Distribution of tophi, bone erosions, and osteophytes. Distribution of tophi based (A) on dual-energy computed tomography as well as bone erosions (B) and osteophytes (C) based on high-resolution peripheral quantitative computed tomography of first metatarsophalangeal (MTP1) joints in patients with gout. Data are shown for the different regions of the MTP1 joint, including the plantar (P), medial (M), dorsal (D), and lateral (L) region of the metatarsal head and phalangeal bases, respectively, as well as the medial sesamoid (MS) and lateral sesamoid (LS) bones. Data indicate percentage of patients with tophi, erosions, and osteophytes in respective region. [Color figure can be viewed at wileyonlinelibrary.com]

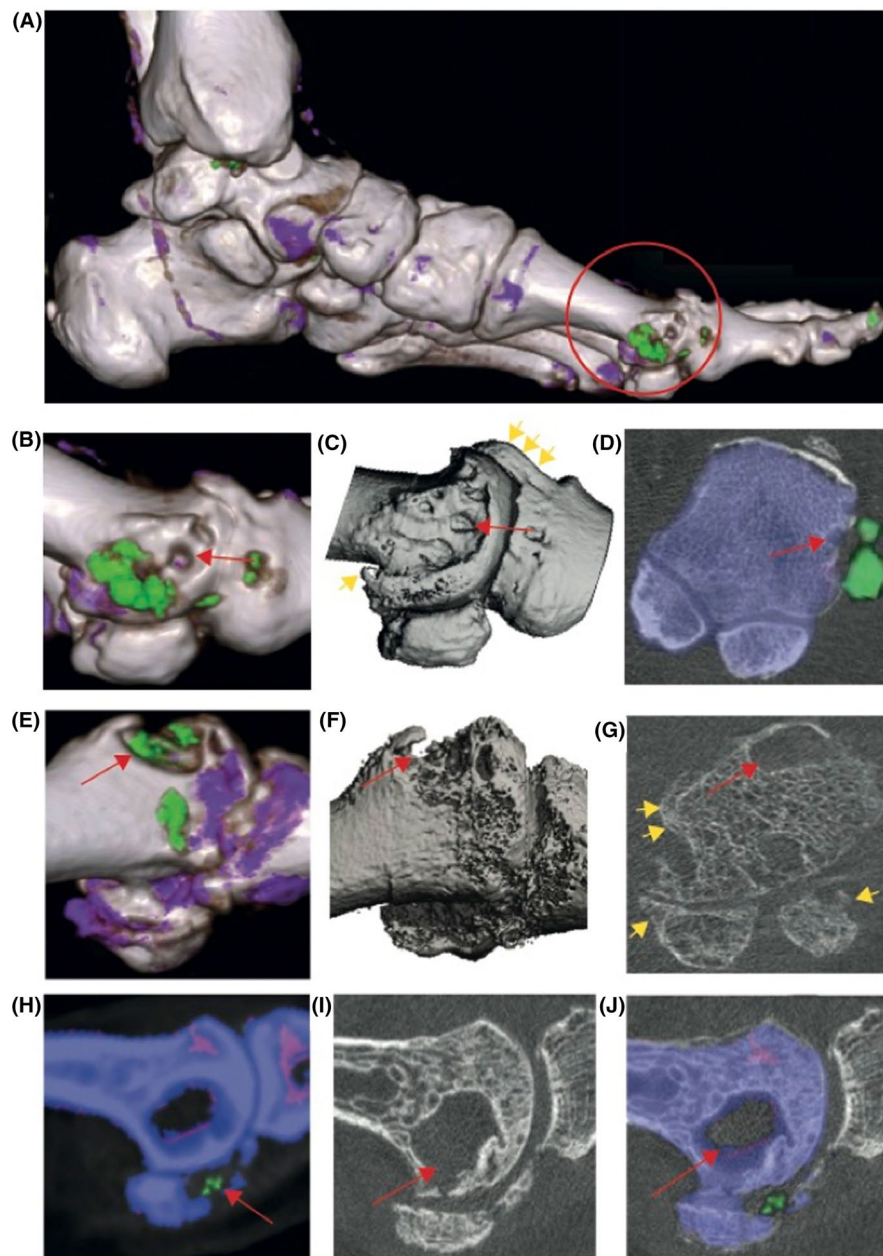


Figure 4. Spatial correlation of tophi and bone erosions. Three examples resembling three patients with gout showing the spatial correlation between tophi detected by dual-energy computed tomography (DECT) and bone erosions detected by high-resolution peripheral quantitative computed tomography (HR-pQCT) in the first metatarsophalangeal (MTP1) joints. First patient: DECT overview of the entire foot of a patient with gout (green lesions in the MTP1 joint and smaller lesion in the ankle joint resemble tophi) (A). Close-up of the DECT result of the MTP1 joint (B), corresponding HR-pQCT (red arrows: erosions; yellow arrows: osteophytes (C), and overlay of DECT and HR-pQCT images showing the intimate relation of tophi and erosions (D). Second patient: DECT image showing tophus (E), corresponding HR-pQCT showing erosion (F), and overlay of DECT and HR-pQCT images (G). Third patient: DECT image showing tophus (H), corresponding HR-pQCT showing erosion (I), and overlay of DECT and HR-pQCT images (J). DECT (A, B, sagittal view) and HR-pQCT (C, sagittal view) images of the first metatarsophalangeal joint of a patient with gout. Green spots (A, B, C) show urate crystal depositions, mainly affecting the medial side of the metatarsal head. Irregular cortical bone pattern is already seen at the area of urate crystal depositions, which can be confirmed as erosive changes by HR-pQCT (C, red arrows) and by fusion images of axial DECT and HR-pQCT images (D). [Color figure can be viewed at wileyonlinelibrary.com]

typically affected joint in gout and is also easily accessible for HR-pQCT scanning. Although DECT and CT studies have been performed in patients with gout, they've shown that the disease is characterized by an erosive burden and that urate deposition

is associated with structural damage; however, the exact special interaction between tophi and bone erosion and osteophytes in vivo has not been assessed (3,5,6,17). Using HR-pQCT, which allows quantitative analysis of peripheral bone using 82- μm voxel

size, we were able to meticulously assess catabolic and anabolic changes and to provide precious data regarding the relationship between urate deposits and bone changes. The comparison with healthy subjects of similar age, sex, and body mass showed that patients with gout have a significantly higher extent of bone damage in the MTP1 joints. Based on the high mechanical burden in the MTP1 joint in humans, comparison of results obtained from patients with gout versus those obtained from healthy controls appears to be important as it allows to exclude that the observed changes are not only due to subclinical osteoarthritis, which is frequent in the MTP1 and also leads to erosions and osteophytes. We found that the extent of bone erosions is higher in patients with gout: Quantification of the bone erosion burden by HR-pQCT revealed that both the number of erosions and the erosion volumes are significantly higher in patients with gout than in healthy controls.

In our study, no significant relationship between erosion volume measured by HR-pQCT and the tophi volume in its vicinity assessed by DECT was found. This finding is in line with those of other authors, who found that urate regression does not lead to an improvement of semiquantitative erosion scoring (18). Our findings are in contrast to those of Shi et al, who showed that erosion volume positively correlates with the volume of urate deposits next to the erosion (9). This divergent results could be explained by the fact that (i) different software for assessing erosion/urate volume were used, (ii) the partial volume defect is larger in DECT, and (iii) HR-pQCT accuracy is based on isotropic voxel size, making it an imaging tool for more in-depth assessment. Longitudinal quantitative studies could be helpful to clarify the relationship between the urate burden and its effect on the erosive volume in the vicinity.

Importantly, osteophytes formation was significantly more pronounced in gout, suggesting that gout leads to a combination of catabolic and anabolic lesion in the bones. Distribution of osteophytes was, however, different from one of the erosions, suggesting that osteophytes resemble more a response of the joint to tophus-induced bone erosion.

Analysis of the MTP1 joint showed a remarkable focal deposition of tophi as well as bone erosions. Both lesions preferentially affect the medial side of the first metatarsal head and, to a somewhat lesser extent, also the medial sesamoid bone and the medial phalangeal base. The reason for the preferential affection of the medial side of the MTP1 joint is not fully clear, but it seems likely the mechanical factors promote the deposition of uric acid crystals. Trauma, for instance, preferentially affects the exposed medial parts of the MTP1 and could lead to local changes in the chemical micromilieu of the tissue facilitating the precipitation of uric acid (19,20).

Simultaneous analysis of tophi by DECT and erosions by HR-pQCT revealed a remarkable special relation between the uric acid deposits and erosions, providing *in vivo* proof of the concept that tophi directly lead to bone erosions. This concept was supported by the similar distribution pattern of tophi and erosions, but

not osteophytes, in the MTP1 joint and the direct colocalization analysis by overlaying DECT and HR-pQCT images. These findings support the data by the Dalbeth group, showing that MSU crystals induce osteoclast formation and suppress osteoblast differentiation, which leads to a local imbalance of bone homeostasis and fosters the generation of bone erosions (21). Furthermore, histological analyses have shown that macrophages reside at the periphery of tophi, providing the source of bone-resorbing osteoclasts and explaining the intimate relation between tophi and erosions (22).

The data also suggest that gout speeds up an osteoarthritic-like remodeling of the joint. Hence, the overwhelming number of patients with gout presented with remarkable osteophytes in the MTP1 joints, which were not found in the healthy controls. In contrast to erosions, however, osteophytes were not directly associated with tophus deposits, which suggests that their formation resembles a repair response to the catabolic effects of MSU crystals on the affected joints.

Our study has some limitations. The cross-sectional study design did not allow us to assess the effect of a urate-lowering therapy on urate deposition and bone erosion over time and only allowed the potential conclusion that urate deposition and erosion in gout occur simultaneously at the same sites. Given the small number of patients, our results should be interpreted cautiously in terms of generalizability and causality, thus future observational studies in larger cohorts are necessary to confirm these results. Another limitation of this study is the difficulty to assess the exact impact of tophi on bone, as DECT only partially determines the tophi extent by measuring urate deposition, with urate corresponding to about 20% of the tophi volume (19). However, our data indirectly indicate that there might be a strong cohesion. Besides the determination of anabolic and catabolic changes, HR-pQCT can be used for the assessment of volumetric bone density and microstructure. This approach was not used in our study, as there is no validated and standardized method for this evaluation so far. Therefore, we have concentrated on the already established evaluation of erosions and osteophytes.

In summary, this study demonstrates a relationship between tophi and structural damage in patients suffering from gout. Showing that there is a direct relation between tophus deposition and bone erosions provides further rationale for the concept that clearance of tophi is of the utmost importance in the treatment of gout by removing the trigger for bone destruction (23).

ACKNOWLEDGMENTS

This study was supported by the German Research Council (DFG: FOR2438/2886; SFB1181), the German Ministry of Science and Education (project MASCARA), the European Union (ERC Synergy grant 4DnanoSCOPE) and EU/EFPIA Innovative Medicines Initiative 2 (project RTCure).

AUTHOR CONTRIBUTIONS

All authors were involved in drafting the article or revising it critically, and all authors approved the final version to be published. Pecherstorfer, Simon, RS, Schett, and Bayat prepared the manuscript, and all listed authors revised the manuscript.

Study conception and design. Pecherstorfer, Simon, Schett, Bayat.

Acquisition of data. Pecherstorfer, Unbehend, Ellmann, Hartmann, Hueber, Haschka, Kleyer, Rech, Bayat.

Analysis and interpretation of data. Pecherstorfer, Simon, Unbehend, Ellmann, Englbrecht, Figueiredo, Kocijan, Rech, Kleyer, Schett, Bayat.

REFERENCES

1. Terkeltaub R. Update on gout: new therapeutic strategies and options. *Nat Rev Rheumatol* 2010;6:30–8.
2. Ragab G, Elshahaly M, Bardin T. Gout: an old disease in new perspective – a review. *J Adv Res* 2017;8:495–511.
3. Dalbeth N, Aati O, Kalluru R, Gamble GD, Horne A, Doyle AJ, et al. Relationship between structural joint damage and urate deposition in gout: a plain radiography and dual-energy CT study. *Ann Rheum Dis* 2015;74:1030–6.
4. Dalbeth N, Clark B, Gregory K, Gamble G, Sheehan T, Doyle A, et al. Mechanisms of bone erosion in gout: a quantitative analysis using plain radiography and computed tomography. *Ann Rheum Dis* 2009;68:1290–5.
5. Dalbeth N, Milligan A, Doyle AJ, Clark B, McQueen FM. Characterization of new bone formation in gout: a quantitative site-by-site analysis using plain radiography and computed tomography. *Arthritis Res Ther* 2012;14:R165.
6. Dalbeth N, Doyle A, Boyer L, Rome K, Survepalli D, Sanders A, et al. Development of a computed tomography method of scoring bone erosion in patients with gout: validation and clinical implications. *Rheumatology (Oxford)* 2011;50:410–6.
7. Dalbeth N, Clark B, McQueen F, Doyle A, Taylor W. Validation of a radiographic damage index in chronic gout. *Arthritis Rheum* 2007;57:1067–73.
8. Shi D, Xu JX, Wu HX, Wang Y, Zhou QJ, Yu RS. Methods of assessment of tophus and bone erosions in gout using dual-energy CT: reproducibility analysis. *Clin Rheumatol* 2015;34:755–65.
9. Shi D, Chen JY, Wu HX, Zhou QJ, Chen HY, Lu YF, et al. Relationship between urate within tophus and bone erosion according to the anatomic location of urate deposition in gout: a quantitative analysis using dual-energy CT volume measurements. *Medicine (Baltimore)* 2019;98:e18431.
10. Stach CM, Bäuerle M, Englbrecht M, Kronke G, Engelke K, Manger B, et al. Periarticular bone structure in rheumatoid arthritis patients and healthy individuals assessed by high-resolution computed tomography. *Arthritis Rheum* 2010;62:330–9.
11. Simon D, Faustini F, Kleyer A, Haschka J, Englbrecht M, Kraus S, et al. Analysis of periarticular bone changes in patients with cutaneous psoriasis without associated psoriatic arthritis. *Ann Rheum Dis* 2016;75:660–6.
12. Geusens P, Chapurlat R, Schett G, Ghasem-Zadeh A, Seeman E, de Jong J, et al. High-resolution in vivo imaging of bone and joints: a window to microarchitecture. *Nat Rev Rheumatol* 2014;10:304–13.
13. Neogi T, Jansen TL, Dalbeth N, Fransen J, Schumacher HR, Berendsen D, et al. 2015 Gout Classification Criteria: an American College of Rheumatology/European League Against Rheumatism collaborative initiative. *Arthritis Rheumatol* 2015;67:2557–68.
14. Bayat S, Aati O, Rech J, Sapsford M, Cavallaro A, Lell M, et al. Development of a dual-energy computed tomography scoring system for measurement of urate deposition in gout. *Arthritis Care Res (Hoboken)* 2016;68:769–75.
15. Figueiredo CP, Kleyer A, Simon D, Stemmler F, d'Oliveira I, Weissenfels A, et al. Methods for segmentation of rheumatoid arthritis bone erosions in high-resolution peripheral quantitative computed tomography (HR-pQCT). *Semin Arthritis Rheum* 2018;47:611–8.
16. Töpfer D, Finzel S, Museyko O, Schett G, Engelke K. Segmentation and quantification of bone erosions in high-resolution peripheral quantitative computed tomography datasets of the metacarpophalangeal joints of patients with rheumatoid arthritis. *Rheumatology (Oxford)* 2014;53:65–71.
17. Towiwat P, Doyle AJ, Gamble GD, Tan P, Aati O, Horne A, et al. Urate crystal deposition and bone erosion in gout: 'inside-out' or 'outside-in'? A dual-energy computed tomography study. *Arthritis Res Ther* 2016;18:208.
18. Dalbeth N, Billington K, Doyle A, Frampton C, Tan P, Aati O, et al. Effects of allopurinol dose escalation on bone erosion and urate volume in gout: a dual energy CT imaging study of a randomized controlled trial. *Arthritis Rheumatol* 2019;71:1739–46.
19. Pascual E, Ordonez S. Orderly arrayed deposit of urate crystals in gout suggest epitaxial formation. *Ann Rheum Dis* 1998;57:255.
20. Roddy E. Revisiting the pathogenesis of podagra: why does gout target the foot?. *J Foot Ankle Res* 2011;4:13.
21. Dalbeth N, Smith T, Nicolson B, Clark B, Callon K, Naot D, et al. Enhanced osteoclastogenesis in patients with tophaceous gout: urate crystals promote osteoclast development through interactions with stromal cells. *Arthritis Rheum* 2008;58:1854–65.
22. Dalbeth N, Pool B, Gamble GD, Smith T, Callon KE, McQueen FM, et al. Cellular characterization of the gouty tophus: a quantitative analysis. *Arthritis Rheum* 2010;62:1549–56.
23. Richette P, Doherty M, Pascual E, Barskova V, Becce F, Castañeda-Sanabria J, et al. 2016 updated EULAR evidence-based recommendations for the management of gout. *Ann Rheum Dis* 2017;76:29–42.